

## $^{41}\text{Ca}$ in Tooth Enamel. Part I: A Biological Signature of Neutron Exposure in Atomic Bomb Survivors

A. Wallner,<sup>a,b,c,1</sup> W. Rühm,<sup>a,d</sup> G. Rugel,<sup>a,b</sup> N. Nakamura,<sup>e</sup> A. Arazi,<sup>b</sup> T. Faestermann,<sup>b</sup> K. Knie,<sup>a,b</sup> H. J. Maier<sup>f</sup> and G. Korschinek<sup>b</sup>

<sup>a</sup> Radiobiological Institute, University of Munich, 80336 Munich, Germany; <sup>b</sup> Faculty of Physics, Technical University of Munich, 85747 Garching, Germany; <sup>c</sup> VERA Laboratory, Faculty of Physics, University of Vienna, 1090 Vienna, Austria; <sup>d</sup> GSF – National Research Center for Environment and Health, 85764 Neuherberg, Germany; <sup>e</sup> Department of Genetics, Radiation Effects Research Foundation, 5-2 Hijiyama Park, Minami-ku, Hiroshima City, 732-0815 Japan; and <sup>f</sup> Faculty of Physics, University of Munich, Am Coulombwall 1, 85748 Garching, Germany

---

Wallner, A., Rühm, W., Rugel, G., Nakamura, N., Arazi, A., Faestermann, T., Knie, K., Maier, H. J. and Korschinek, G.  $^{41}\text{Ca}$  in Tooth Enamel. Part I: A Biological Signature of Neutron Exposure in Atomic Bomb Survivors. *Radiat. Res.* 174, 137–145 (2010).

The detection of  $^{41}\text{Ca}$  atoms in tooth enamel using accelerator mass spectrometry is suggested as a method capable of reconstructing thermal neutron exposures from atomic bomb survivors in Hiroshima and Nagasaki. In general,  $^{41}\text{Ca}$  atoms are produced via thermal neutron capture by stable  $^{40}\text{Ca}$ . Thus any  $^{41}\text{Ca}$  atoms present in the tooth enamel of the survivors would be due to neutron exposure from both natural sources and radiation from the bomb. Tooth samples from five survivors in a control group with negligible neutron exposure were used to investigate the natural  $^{41}\text{Ca}$  content in tooth enamel, and 16 tooth samples from 13 survivors were used to estimate bomb-related neutron exposure. The results showed that the mean  $^{41}\text{Ca}/\text{Ca}$  isotope ratio was  $(0.17 \pm 0.05) \times 10^{-14}$  in the control samples and increased to  $2 \times 10^{-14}$  for survivors who were proximally exposed to the bomb. The  $^{41}\text{Ca}/\text{Ca}$  ratios showed an inverse correlation with distance from the hypocenter at the time of the bombing, similar to values that have been derived from theoretical free-in-air thermal-neutron transport calculations. Given that  $\gamma$ -ray doses were determined earlier for the same tooth samples by means of electron spin resonance (ESR, or electron paramagnetic resonance, EPR), these results can serve to validate neutron exposures that were calculated individually for the survivors but that had to incorporate a number of assumptions (e.g. shielding conditions for the survivors). © 2010 by Radiation Research Society

### INTRODUCTION

The cohort of atomic bomb (A-bomb) survivors in Hiroshima and Nagasaki provides a major source of information on health effects after exposure to ionizing

<sup>1</sup> Address for correspondence: VERA Laboratory, Faculty of Physics, University of Vienna, Währinger Strasse 17, A-1090 Wien, Austria; e-mail: anton.wallner@univie.ac.at.

radiation (1–3). Since the beginning of the Life Span Study (LSS) at the Atomic Bomb Casualty Commission (ABCC) and subsequently at the Radiation Effects Research Foundation (RERF), approximately 93,000 survivors exposed to various doses of radiation as well as 27,000 individuals who were not in Hiroshima or Nagasaki at the time of the bombings have been monitored continuously to document cancer mortality, cancer incidence and cause of death to assess the impacts of radiation on human health. To verify a correlation between any suspected health effect associated with radiation exposure, however, individual dose assessments for each of the survivors are essential. These efforts are currently conducted through the use of sophisticated computer calculations based on interview information regarding exposure conditions at the time of the bombings. However, dose estimates include various degrees of uncertainties because the radiation fields in Hiroshima and Nagasaki were complicated and characterized by two components—neutron and  $\gamma$  radiation. In addition, various parameters such as the degree of shielding and distance from the point of explosion make the quantification of individual doses a rather complicated issue.

In the past, several dosimetry systems have been developed to estimate individual doses as well as organ doses [T57D (4), T65D (5), DS86 (6) and DS02 (7)]. However, these calculations and their associated uncertainties need to be verified experimentally, and verification of neutron exposure becomes increasingly difficult over the years for several reasons, most notably due to the spontaneous decay of neutron-activated radionuclides.

To illustrate this decay problem, one project started a few days after the explosions and involved the collection of samples containing sulfur that contained short-lived  $^{32}\text{P}$  ( $t_{1/2} = 14.3$  days) produced via the fast-neutron-induced reaction  $^{32}\text{S}(n,p)^{32}\text{P}$ . This was used to reconstruct the fast-neutron fluence close to the hypocenter in

Hiroshima (8–10). Over the following years, various other longer-lived reaction products such as  $^{60}\text{Co}$ ,  $^{152}\text{Eu}$  and  $^{36}\text{Cl}$  with half-lives ranging from 5 years to 300,000 years were (and still are being) measured [see ref. (11) for a detailed list of references]. These products are almost exclusively the result of thermal-neutron exposure. Recently, efforts have been made to measure fast neutrons using the  $^{63}\text{Cu}(n,p)^{63}\text{Ni}$  reaction ( $^{63}\text{Ni}$ :  $t_{1/2} = 101$  years) (12–17) and the  $^{39}\text{K}(n,p)^{39}\text{Ar}$  reaction [ $^{39}\text{Ar}$ :  $t_{1/2} = 269$  years; see ref. (18)] at distances from the hypocenter where people could survive, and these results were in close agreement with calculated values in the investigated samples. In addition, new measurements of thermal-neutron-induced  $^{36}\text{Cl}$  also showed a reasonable agreement with the DS02 calculations (19–24), even at distances beyond 1,000 m from the hypocenter where previous studies found poor agreement with neutron transport calculations (25, 26).

All these studies were based on inorganic sample materials taken from locations such as buildings that survived the A-bomb blast and the fires that followed the bombing. Both directly exposed and shielded samples were used. Because of the limited number of suitable samples and the complexity of the applied detection methods, however, neutron fluences could not be reconstructed experimentally for the individual locations where the majority of the survivors in the epidemiological study cohort (LSS) were exposed. In addition, most of the neutron measurements were done on radionuclides produced by thermal neutrons, which provide only an indirect signature of the fast neutrons. Thus all efforts to date to reconstruct the neutron exposure of the survivors remain indirect and require extrapolation from experimentally reconstructed neutron fluences to the locations where people survived and to neutron energies and doses that were responsible for biological effects.

In the present work, a method is described that allows a more direct reconstruction of the survivors' neutron exposure. Specifically, it is suggested that the long-lived radionuclide  $^{41}\text{Ca}$  ( $t_{1/2} = 103,000$  years) in the tooth enamel of the survivors is used for dosimetry purposes. This radionuclide was produced by thermal neutrons originating from the A-bomb radiation. In a selected number of tooth samples, individual  $^{41}\text{Ca}$  concentrations were measured by means of accelerator mass spectrometry (AMS), and these measurements are described in detail below. The results obtained for tooth enamel samples exposed to A-bomb neutrons are compared to samples that were not exposed to a significant dose of A-bomb neutrons. For the exposed samples, a significant inverse correlation was found between the distance from the hypocenter in Hiroshima and the amount of  $^{41}\text{Ca}$  measured. Such data provide a key quantity in neutron dosimetry, because these results do not depend on the accuracy of survivor recall, e.g. distance and shielding conditions.

**TABLE 1**  
**Production of  $^{41}\text{Ca}$  in Hiroshima, Based on DS02**  
**Calculations 1 m above the Ground and without**  
**Intervening Shielding (5)**

Ground range (m)	800	900	1000	1100	1200	1300
$^{41}\text{Ca}/\text{Ca}$ ratio (in $10^{-15}$ )	55	23	12	5.3	2.5	1.2

## MATERIALS AND METHODS

### *Natural Production of $^{41}\text{Ca}$*

$^{41}\text{Ca}$  is produced almost exclusively via the capture of neutrons by stable  $^{40}\text{Ca}$ , and these neutrons originate from the interaction of primary cosmic radiation with atmospheric components. Typically,  $^{41}\text{Ca}/\text{Ca}$  isotope ratios of about  $6 \times 10^{-15}$  are expected on the surface of the Earth if saturation was achieved and Earth surface erosion processes are neglected [calculated according to ref. (27)]. If erosion occurs, a sample that had been shielded against cosmic radiation for most of the time now appears on the Earth's surface and would have somewhat lower  $^{41}\text{Ca}/\text{Ca}$  isotope ratios. Near the geomagnetic poles, however, the shielding of the cosmic rays by the magnetic field of the Earth is less effective, and higher ratios are expected. Thus the actual  $^{41}\text{Ca}/\text{Ca}$  ratio found in the lithosphere depends on the geographic area (28, 29). Through erosion processes,  $^{41}\text{Ca}$  is distributed into different compartments of the global ecosystem and finally enters the food chain. Therefore,  $^{41}\text{Ca}/\text{Ca}$  isotope ratios will also be found in the human body. As a result,  $^{41}\text{Ca}/\text{Ca}$  isotope ratios in inorganic or biological materials are expected to vary somewhat depending on the region where the specific sample was found. In fact, values as low as  $6 \times 10^{-16}$  and as high as  $2 \times 10^{-14}$  have been reported [see ref. (28) for a review].

### *Estimation of $^{41}\text{Ca}$ Production by Neutrons from the Bomb*

To calculate the neutron exposure of A-bomb survivors, the DS02 model considers the propagation of the neutrons produced by the A-bomb explosion through the atmosphere to the ground. Based on these calculations and the ENDF/B-VI production cross-section (30), the  $^{41}\text{Ca}$  content in samples containing stable  $^{40}\text{Ca}$  can be estimated. To provide a first estimate, Table 1 shows  $^{41}\text{Ca}/\text{Ca}$  isotope ratios that were calculated based on DS02 neutron fluences at a height of 1 m and free-in-air (i.e. without shielding) for different distances from the hypocenter in Hiroshima (7). Because the cross-section is largest at low energies, thermal neutrons dominate in the production of  $^{41}\text{Ca}$ . In fact, based on DS86 neutron spectra from Hiroshima, neutrons with energies below 10 keV account for more than 99% of the  $^{41}\text{Ca}$  production at a distance of 1,000 m from the hypocenter.

### *Calcium in the Human Body*

Based on the reference man defined by the International Commission on Radiological Protection, calcium accounts for 1.6% for males and 1.4% for females, respectively, of the total body weight (31). In absolute terms, this corresponds to about 1,000 g of calcium, most of which is bound to the skeleton (99%). Specifically, 13 g of calcium is concentrated in human teeth, and the concentration is highest in the tooth enamel (36%). In addition, enamel shows the highest inorganic fraction within the body. Approximately 1 g of calcium is incorporated daily via ingestion, and about 30% is absorbed by the body. After dentition is finished, however, tooth enamel represents a nearly closed system, tooth calcium metabolism is strongly reduced, and exchanges with natural calcium are negligible [see e.g.  $^{90}\text{Sr}$  investigations in enamel in refs. (32, 33)].

### *Tooth Enamel*

In the present study, 16 tooth samples from 13 survivors who were proximally exposed to A-bomb neutrons (<1,200 m from the

hypocenter) were examined. From three of the survivors, two different teeth were investigated to test the variability of  $^{41}\text{Ca}/\text{Ca}$  ratios in different teeth from the same donor. The results were compared to those obtained from six survivors in a control group (estimated total  $\gamma$ -ray plus neutron doses of  $<5$  mGy were calculated using the DS02). All tooth samples were extracted for medical reasons and were donated by the survivors.

The research plan for this study was approved by the Human Investigation Committee and the Ethics Committee of the Radiation Effects Research Foundation.

#### AMS Sample Preparation

The AMS technique used in the present study requires the use of negative ion sputter sources: Sample material, inserted into an ion source, is sputtered, and negatively charged ions are extracted and analyzed for their mass and energy. Therefore, the original sample material must be converted into a chemical form that readily forms negative ions.

Generally, isobars (i.e., isotopes having the same mass as the isotope of interest) represent a major contribution to background signals when mass spectrometry techniques are applied. In the case of  $^{41}\text{Ca}$ , the interfering isobar is stable  $^{41}\text{K}$  having a mass difference from  $^{41}\text{Ca}$  of only 0.007%, and such a small difference is difficult to resolve by mass spectrometry. Unfortunately, potassium forms negative ions more effectively than calcium, and the  $^{41}\text{K}$  signal would be far stronger than that of  $^{41}\text{Ca}$  if elemental calcium with some potassium impurities were used. Because of the very low isotope ratios expected to be present in the exposed samples (see Table 1), an effective isobar suppression method is essential for this type of study. Therefore, it was decided to convert the enamel material to calcium hydride ( $\text{CaH}_2$ ) as described previously (34). From this material, high currents of negative  $\text{CaH}_3^-$  can be extracted from the ion source and the corresponding  $\text{KH}_3$  molecules do not form negative ions (35, 28). Despite the complicated procedures required for sample preparation, this method was adopted because of its effectiveness in suppressing the isobar signal already in the ion source.

The conversion of enamel into AMS samples was performed as described earlier (36). Briefly, enamel was mechanically separated from dentin and crushed into small particle sizes for ESR measurements (37). The samples were then dissolved in nitric acid. Under controlled pH conditions, calcium precipitated as Ca-oxalate ( $\text{CaC}_2\text{O}_4$ ) in the presence of ammonia and oxalic acid.  $\text{CaC}_2\text{O}_4$  was ignited at  $900^\circ\text{C}$  and fully converted to oxides ( $\text{CaO}$ ). After reduction to metallic calcium at a temperature of  $1,400^\circ\text{C}$ , the addition of hydrogen at a temperature of  $630^\circ\text{C}$  led to the production of calcium-hydride ( $\text{CaH}_2$ ). The chemical procedures of reduction and hydrogenation used have been described (34, 38, 39). This procedure resulted in an overall efficiency of calcium recovery of about 90%. Finally,  $\text{CaH}_2$  material was mixed with a silver powder for better thermal and electrical conductivity, and a few milligrams of this material was then pressed into copper sample holders. This last step was done in an argon atmosphere because  $\text{CaH}_2$  is strongly hygroscopic.

#### AMS Measurements

The  $^{41}\text{Ca}/\text{Ca}$  isotopic ratios in 22 tooth enamel samples were measured at the AMS facility in Munich, Germany, with a few samples also measured at the VERA facility in Vienna, Austria. These systems allow detection of  $^{41}\text{Ca}/\text{Ca}$  levels below  $1 \times 10^{-15}$ . In the following, the measurement procedure is demonstrated by the Munich facility: Negative  $^{41}\text{CaH}_3^-$  ions are produced in a cesium sputter source and are pre-accelerated and pass through a low-energy mass spectrometer that is adjusted for a mass of 44. The ions are then further accelerated and injected into a tandem accelerator (typical tandem voltage: 12.7 MV). Any molecules that might contribute to molecular interference (with mass 44) are completely destroyed in the

terminal stripper foil of the accelerator. The stripper is responsible for charge exchange and produces positively charged ions. After exiting the tandem accelerator,  $^{41}\text{Ca}^{10+}$  ions are selected by a  $90^\circ$  analyzing magnet for further transport to the detector. The particles have an energy of about 140 MeV. Rejection of isotopic interference from  $^{40}\text{Ca}$  and  $^{42}\text{Ca}$  atoms was achieved with a Wien filter and a time-of-flight system. Further reductions of any isobaric and isotopic interference were achieved by means of a GAMS (gas-filled analyzing magnet system) detection system that consists of a gas-filled magnet (GFM) and a position sensitive multi-delta-E ionization chamber. In the GFM, the incoming ions undergo collisions with the gas molecules and as a result reach an equilibrium charge state that depends on the nuclear charge of the incoming ions. Due to the magnetic field, ions from different isobars follow different trajectories and can be separated in the position-sensitive ionization chamber. In the detector, besides the position, the total energy and five energy-loss signals from the incoming ions are also measured. This system is described in refs. (40) and (41), and its application for the detection of  $^{41}\text{Ca}$  is described in detail in ref. (36); the second AMS facility used, VERA, is based on a 3-MV tandem accelerator and is equipped with a dedicated ionization chamber with high energy resolution for  $^{41}\text{Ca}$  detection (42, 43). This setup provides isotopic and isobaric suppression also for medium-mass isotopes: For  $^{41}\text{Ca}$  detection, mainly due to use of  $^{41}\text{CaH}_3^-$  ions, a substantially reduced background of  $^{41}\text{K}$  is observed. Residual particles entering the detector are separated in energy due to their different energy loss in the detector entrance foil and the detector gas ( $\Delta E/E$  detector). Energy loss and residual energy are measured via a segmented anode [for more details, see ref. (43)].

To illustrate the entire detection process, Fig. 1 shows typical spectra obtained from a standard with a known  $^{41}\text{Ca}/\text{Ca}$  ratio of  $10^{-11}$  and from a sample with an isotope ratio of  $4 \times 10^{-15}$ . Figure 1a depicts all the accumulated events during a measurement run. The area of expected  $^{41}\text{Ca}$  signals is indicated by the solid contour line. The dense area below the region of interest stems from  $^{42}\text{Ca}$ -generated events that are still able to find their way to the detector. Figure 1b shows the final events generating these data when combined with the information from all the other signals. The  $^{42}\text{Ca}$  events are completely rejected while most of the  $^{41}\text{Ca}$  events are still accepted.  $^{40}\text{Ca}$  or  $^{42}\text{Ca}$  currents are measured with Faraday cups positioned along the beamline. The ratio of the  $^{41}\text{Ca}$  Ca count rate measured with the detector, and the stable calcium particle rates deduced from the current measurement gives the  $^{41}\text{Ca}/^{40}\text{Ca}$  and  $^{41}\text{Ca}/^{42}\text{Ca}$  isotope ratios.

To monitor particle transmission through the overall system, standards with known  $^{41}\text{Ca}/\text{Ca}$  isotope ratios are measured at certain intervals (36). Typically, a transmission of several percent can be achieved; i.e., out of 100  $^{41}\text{Ca}$  ions injected into the tandem accelerator, depending on the measurement setup used, between 3 to 20  $^{41}\text{Ca}$  nuclei are finally detected. Losses are due to the transport of the ions from the entrance of the accelerator to the detector, the stripping yield to the positive charge state  $10^+$  when passing the terminal foil of the accelerator, and also software data reduction when analyzing the detector spectra. If normalized to the ion current after leaving the tandem accelerator, the corresponding detection efficiency was about 40%.

The  $^{41}\text{Ca}/\text{Ca}$  ratio in a sample of interest is calculated from the  $^{41}\text{Ca}$  events in the detector and the number of stable calcium ions injected into the system that were measured by means of a Faraday cup. If a sample was measured several times during independent runs, the final  $^{41}\text{Ca}/\text{Ca}$  ratio can be obtained by calculating the weighted average of the individual results.

In addition, although it is rather unlikely in the experimental setups used, another ion may mimic a true  $^{41}\text{Ca}$  event in the detector, and the possibility that some contamination during the chemical preparation or present in the ion source could affect the low measured  $^{41}\text{Ca}/\text{Ca}$  ratio cannot be excluded. To quantify or exclude such possible background contributions, blank or control samples were also

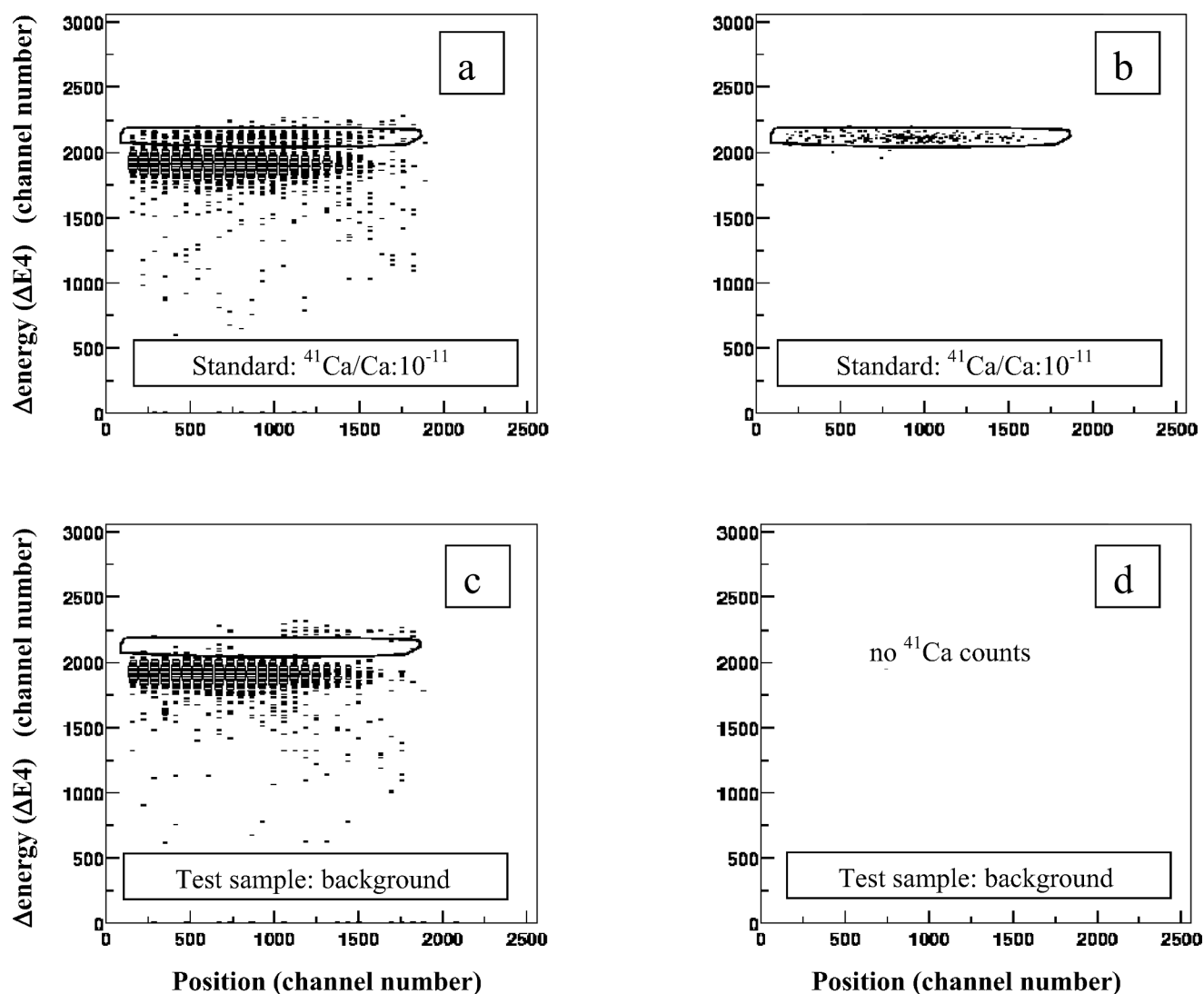


FIG. 1. Panels a and b: Typical spectra of a standard with a ratio of  $^{41}\text{Ca}/\text{Ca} \approx 10^{-11}$  in terms of one energy loss signal from the detector (ordinate) relative to the position in the detector (abscissa); for details see text. Panels c and d: Typical spectra of a background sample with a ratio of  $^{41}\text{Ca}/\text{Ca} < 4 \times 10^{-15}$  in terms of one energy loss signal,  $\Delta E4$ , from the detector (ordinate) relative to the position in the detector (abscissa).

measured. Pure blank samples (commercially available  $\text{CaH}_2$  with an unknown but low natural  $^{41}\text{Ca}/\text{Ca}$  ratio) as well as so-called chemical blanks were used. The latter had to undergo the same chemical preparation steps as the experimental samples and were also measured repeatedly to obtain information on possible machine or chemistry background events. Importantly, the tooth samples from the survivors in the control group were used to evaluate the natural background ratio. Table 2 summarizes parameters that are typical for the preparation of the enamel samples and the  $^{41}\text{Ca}$  AMS measurements.

#### Estimation of Uncertainty

Uncertainties (in this paper, these are expressed at the  $1\sigma$  level) are given in a summary table for the individual samples (Table 3) and include all sources. Because of the limited number of counts detected (between 17 and 64 counts of  $^{41}\text{Ca}$  per sample), the uncertainty due to Poisson counting statistics was between 13% and 24%. Measurement of the transmission through the system (which was performed by using standard samples) represented an additional source of uncertainty. While the uncertainty from Poisson statistics for these measurements was usually negligible, uncertainties from fluctuations

TABLE 2  
Typical Parameters Used for the  $^{41}\text{Ca}$  AMS  
Measurements of the Tooth Samples

Typical parameters in $^{41}\text{Ca}$ -AMS		
Total mass of enamel sample	60–200 mg	
Total mass of calcium in enamel	22–70 mg	
Sample mass per cathode	a few mg	
Sample material	$\text{CaH}_2$	
Ion currents ( $\text{CaH}_3^-$ )	0.3–5 $\mu\text{A}$	
	Munich	Vienna
Terminal voltage	12.5–13 MV	3 MV
Charge state after tandem	$10^+$	$4^+$
Transmission	3–5%	25%
Particle energy	140 MeV	15 MeV

*Note.* Transmission is defined as the fraction of particles, which is identified by the detector from the particles injected into the accelerator.

**TABLE 3**  
Sources of Uncertainties Considered to Contribute to the Total Uncertainty of the Final Isotope Ratios

Uncertainty contribution	Type of error	
Poisson statistics	R	13–24%
Particle current	R	6%
Reproducibility of standards	R	5%
Absolute value of standards	S	10%
Uncertainty of background ratio	S	5–40%
Total uncertainty for exposed samples		20–49%

*Note.* R indicates random types of uncertainty contributions, and S indicates systematic types of uncertainty contribution.

in the particle current due to instabilities in the machine as well as long-term drifts in the overall transmission current contributed more significantly. This uncertainty is considered random and was typically 4–6%. Besides random errors, systematic uncertainties were also considered. For example, for the determination of the absolute isotope ratio of the unknown samples, the uncertainty of the <sup>41</sup>Ca/Ca ratio of the standard sample material has to be taken into account, and this was estimated to be 10%. In addition, the uncertainty of the background ratio ( $0.5 \times 10^{-15}$ ) contributes a systematic uncertainty to the net absolute value of the unknown ratios.

Table 3 summarizes these contributions. Because they are considered uncorrelated, the total uncertainty given in Table 5 for the exposed samples was calculated by applying the Gaussian law of error propagation. Although considerable efforts were made to quantify the background, the uncertainty contribution still dominates the uncertainty of the lower measured <sup>41</sup>Ca/Ca ratios. For samples with higher measured <sup>41</sup>Ca/Ca ratios, both systematic and random contributions are similar.

**TABLE 5**  
Summary of the Exposed Tooth Samples

Sample ID <sup>a</sup>	Tooth position <sup>b</sup>	Gamma-ray dose in tooth <sup>c</sup>	Ground range (m) <sup>f</sup>	Counts <sup>41</sup> Ca	T <sub>M</sub> (h)	<sup>41</sup> Ca/Ca ratio (in 10 <sup>-15</sup> )	
						Measured value	Background corrected data
F04	7	3.1 Gy	827	64	12	21 ± 3	19.5 ± 4.0
H43	6	2.5 Gy	884	40	14	15 ± 1	13.5 ± 2.0
E90	1	2.3 Gy	894	26	9	19 ± 4	16.9 ± 4.1
G91	7(RU) <sup>d</sup>	3.1 Gy	952	53	8	13 ± 2	11.3 ± 2.3
G65	6(LU) <sup>d</sup>	2.7 Gy	952	55	11	11 ± 2	9.1 ± 2.0
A72	2(LU) <sup>d</sup>	3.6 Gy	956	44	11	20 ± 3	18.2 ± 4.0
A34	3(RU) <sup>d</sup>	3.9 Gy	956	37	7	20 ± 3	18.5 ± 4.0
M93	8	1.2 Gy	1000	44	16	9 ± 2	7.2 ± 2.5
K67	6	1.2 Gy	1018	29	12	7 ± 1	5.0 ± 1.5
D20	7	2.7 Gy	1057	17	7	10 ± 3	8.6 ± 2.7
I29	8	1.8 Gy	1108	24	21	6 ± 2	3.9 ± 2.0
B51	4(RU) <sup>d</sup>	2.4 Gy <sup>e</sup>	1111	24	9	9 ± 2	7.4 ± 2.1
B53	4(LL) <sup>d</sup>	2.4 Gy <sup>e</sup>	1111	17	11	9 ± 2	7.5 ± 2.4
L80	7/8	1.7 Gy	1116	53	10	9 ± 2	7.6 ± 2.0
C47	8	2.8 Gy	1124	17	10	8 ± 2	6.0 ± 2.1
J66	7	1.2 Gy	1163	23	14	5 ± 2	2.8 ± 3.0

*Notes.* Uncertainties in background corrected data include all uncertainty contributions (see text). The isotope ratios are given in units of 10<sup>-14</sup>.

<sup>a</sup> The survivor IDs are the same as described in the previous report in which the ESR measurements of  $\gamma$ -ray doses were described (37).

<sup>b</sup> 1 and 2 = incisor, 3 = canine, 4 = bicuspid, 6–8 = molar.

<sup>c</sup> The doses were estimated by ESR from lingual part of the samples, otherwise noted.

<sup>d</sup> LU = left upper jaw, RU = right upper jaw, LL = left lower jaw.

<sup>e</sup> Molar dose from the same donor.

<sup>f</sup> Ground ranges were individually deduced by means of a customized approach described in ref. (51).

**TABLE 4**  
<sup>41</sup>Ca/Ca Isotope Ratios (in units of 10<sup>-15</sup>) Obtained from Samples from Survivors in the Control Group

Sample number (ID)	Counts	T <sub>M</sub> (h)	<sup>41</sup> Ca/Ca ratio (in 10 <sup>-15</sup> )		
				+1 $\sigma$	-1 $\sigma$
1 (R408)	3	11	1.5	1.2	1.0
2 (R196)	10	17	2.6	1.0	0.8
3 (R556)	1	10	1.0	1.7	0.6
4 (R621)	3	10	4.7	3.6	3.0
5 (R556-2)	0	6	0.0	1.4	0.0
6 (R577)	3	4	2.1	1.6	1.4
All controls	20	59	1.7	0.5	0.5

*Notes.* Listed are the total <sup>41</sup>Ca counts detected, total measuring time T<sub>M</sub>, and the measured isotope ratios. Given errors include only uncertainties due to Poisson statistics (44).

## RESULTS AND DISCUSSION

### Control Samples

Five tooth samples from six survivors in the control group in Hiroshima were measured repeatedly. In all cases, the number of <sup>41</sup>Ca events detected was low, and the total number of counts per sample was between 0 and 10 counts (Table 4).

Figure 2 shows the individual ratios obtained from the AMS measurements. Due to the low number of counts obtained from these samples, the error bars are dominated by the uncertainty due to Poisson counting statistics. Also shown are the weighted mean back-

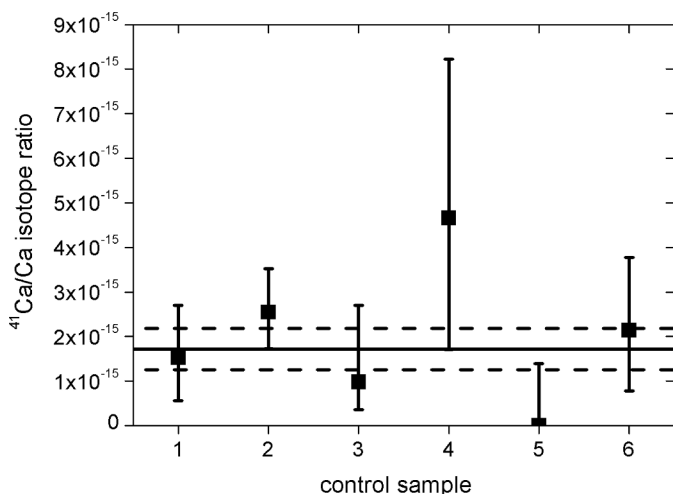


**FIG. 2.** AMS results for the six samples that were not significantly exposed to A-bomb neutrons (symbols). The error bars depict the statistical errors only. The solid horizontal line gives the weighted mean ratio, the dashed lines the  $1\sigma$ -standard deviation of the mean value. Samples 3 and 5 were from the same donor (see Table 4).

ground ratio (solid horizontal line) and the  $1\sigma$ -standard deviation of the mean (dashed lines).

Overall, for background control values, 20 counts were recorded in 59 h of measuring time. The weighted mean  $^{41}\text{Ca}/\text{Ca}$  ratio of the six individual results is  $(1.72 \pm 0.46) \times 10^{-15}$ . The error is the standard deviation of the weighted mean. If it is assumed that all samples showed an identical isotope ratio, i.e., if the scattering of the data reflects only statistical measurement uncertainties, then the results summarized in Table 4 can be interpreted as being obtained from one single measurement with 20 counts. In this case a mean background value of  $(2.0 + 0.5/-0.4) \times 10^{-15}$  is obtained, which is consistent with the result of  $(1.72 \pm 0.46) \times 10^{-15}$  given above. The given individual uncertainty includes only statistical uncertainty and was calculated by applying the Poisson uncertainty determination (44). The comparison of external (standard deviation of the mean) and internal uncertainties (Poisson statistics) shows that at this level, no significant additional uncertainty contributions to the obtained background value were observed.

To summarize, the  $^{41}\text{Ca}/\text{Ca}$  isotope ratios obtained in these samples were consistently low and  $\approx 1.7 \times 10^{-15}$  (Table 4). Because some background contributions from chemistry and measurement techniques cannot be excluded, this ratio represents an upper limit for the  $^{41}\text{Ca}/\text{Ca}$  ratio occurring naturally in the Hiroshima area. In the following sections, a background value of  $(1.7 \pm 0.5) \times 10^{-15}$  is used for the correction of the samples exposed to A-bomb neutrons.

#### Exposed Samples

Table 5 summarizes the  $^{41}\text{Ca}/\text{Ca}$  isotope ratios obtained from tooth samples from the survivors who were

exposed to the bomb and stayed within 1,200 m (between 827 m and 1163 m) of the hypocenter. These results showed significantly higher ratios than those obtained from the control cases (Table 4). Table 5 also includes information on tooth position, distance from the hypocenter, number of  $^{41}\text{Ca}$  events identified in the detector, and total time of measurement (in hours). The  $^{41}\text{Ca}/\text{Ca}$  ratio given for individual samples was calculated from results obtained during several runs using Eq. ((2)). Finally, for each tooth sample, the net result was obtained by subtracting the background value of  $(1.7 \pm 0.5) \times 10^{-15}$  (Table 4, last line).

#### Advantage of AMS for Studies on Neutron Exposure from A-Bomb

As mentioned earlier,  $^{41}\text{Ca}/\text{Ca}$  isotope ratios expected in samples exposed to A-bomb neutrons or to secondary neutrons from cosmic radiation are of the order of  $10^{-15}$  to  $10^{-14}$ . Because about 50 mg of calcium was available on average for each tooth sample, a typical sample contains about  $10^6$  to  $10^7$   $^{41}\text{Ca}$  atoms. Given a half-life of 103,000 years (45, 46), this corresponds to radioactivities of about 0.1 to a few  $\mu\text{Bq}$ , which is far below the detection limit of decay-counting techniques. Therefore, only atom-counting methods can be applied for this type of study, and it is for this reason that the AMS technique was used in the present study for the detection of  $^{41}\text{Ca}$ .

The application of the Munich MP tandem accelerator to detect  $^{41}\text{Ca}$  produced by A-bomb neutrons has already been demonstrated in an earlier study [a general description of  $^{41}\text{Ca}$ -AMS is given elsewhere (28, 47, 48)]. In this study, a  $^{41}\text{Ca}$  profile was measured in a granite gravestone exposed to neutrons from the bomb at close distances from the hypocenter in Hiroshima (49, 50). More recently, an improved AMS setup was installed featuring a GFM (40). This setup is characterized by a much lower  $^{41}\text{Ca}$  detection limit and therefore allows  $^{41}\text{Ca}$  measurements to be made in survivors who were exposed at longer distances from the hypocenter in Hiroshima where they could survive the explosion. In addition, recent improvements allow the detection of  $^{41}\text{Ca}$  in environmental samples with  $^{41}\text{Ca}/\text{Ca}$  levels even below  $10^{-15}$  (36, 43).

#### Specific Characteristics of AMS Analysis of Tooth Enamel

The overall detection efficiency at the AMS laboratories, which includes the machine transmission, the efficiency for producing negative ions in the ion source [ $\approx 0.2\%$  (28)], and the chemistry yield, is of the order of a few  $\times 10^{-4}$ . If a typical enamel sample is considered with a mass of 100 mg, i.e. 36 mg calcium, and a  $^{41}\text{Ca}/\text{Ca}$  isotope ratio of  $5 \times 10^{-15}$ , about  $3 \times 10^6$   $^{41}\text{Ca}$  atoms would be present. The value of  $1-3 \times 10^{-4}$  for the overall efficiency would then correspond to a total number of

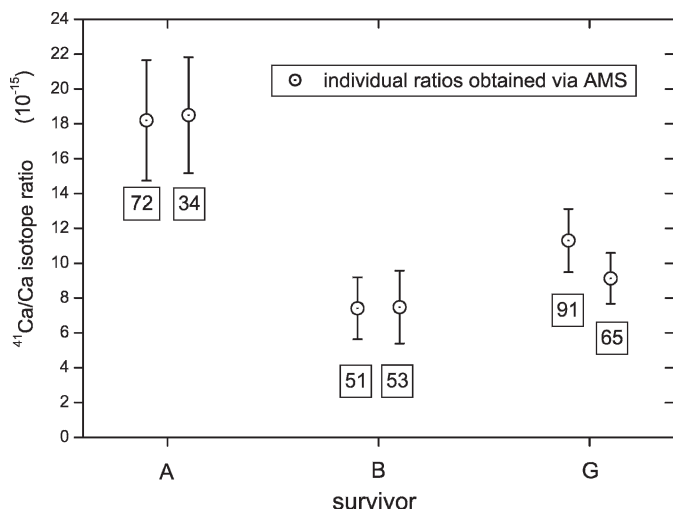


FIG. 3. Results of <sup>41</sup>Ca/Ca AMS measurements obtained from survivors who donated two teeth. The numbers in the boxes represent the sample-ID numbers in Table 5.

about 300 to 1000 <sup>41</sup>Ca atom counts, which in principle can be detected with AMS if all of the sample material is completely sputtered (this would correspond to a measuring period of about 25 h).

It should be noted that, due to the observed background, the applicability of the proposed method is limited to a ground range of less than about 1,200 m from the bomb hypocenter. For those who survived at greater distances, the <sup>41</sup>Ca/Ca ratio induced by A-bomb neutrons is expected to be smaller than the background ratio measured (Table 1).

*Intertooth Variation in the Same Survivors*

To assess the reproducibility of the AMS measurements, intertooth variation of the induced <sup>41</sup>Ca/Ca ratio was measured by examining two teeth from the same survivor (performed for a total of three survivors and indicated by letter descriptors in the first column of Table 5). The results of the two measured ratios for each survivor were in close agreement (Fig. 3), which was better than expected from the uncertainty estimated for individual measurements. Although the number of samples tested was limited, the results indicate that the AMS method produces consistent results and that the <sup>41</sup>Ca signals induced by thermal neutrons from the bomb do not differ extensively among the different teeth in the mouth (cf. two molars from donor G; one was on the right side and the other on the left side of the donor's mouth).

*<sup>41</sup>Ca Yield in Relation to Distance from the Hypocenter*

The present report confirms earlier studies that found evidence for a significantly higher <sup>41</sup>Ca signal in enamel from one exposed survivor (36). To further demonstrate that the observed <sup>41</sup>Ca signal is primarily attributable to

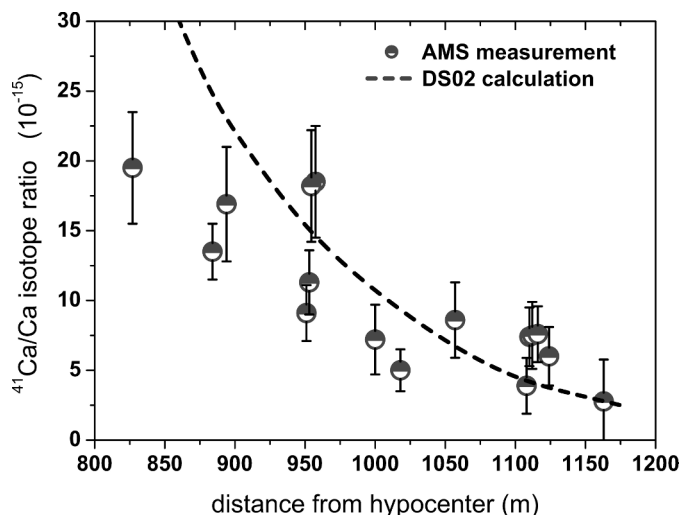


FIG. 4. Decrease of <sup>41</sup>Ca/Ca ratios with distance from the hypocenter. For comparison, DS02 calculations (dashed line) are shown, which were calculated without taking individual shielding conditions into account (free-in-air kerma dose, 1 m above ground; see Table 1). The error bars include all sources of uncertainties. A detailed comparison between measured and calculated <sup>41</sup>Ca/Ca ratios including the individual shielding situation of the survivors is given in ref. (51).

neutron exposure from the bomb, the background-corrected <sup>41</sup>Ca/Ca isotope ratios (Table 5) were plotted as a function of distance from the hypocenter (Fig. 4). A clear trend of decreasing signals with increasing distance is observed. The measured data indicate a slightly lower decrease in <sup>41</sup>Ca production with distance to the hypocenter compared to DS02. Because the latter does not directly calculate the individual shielding conditions, a more quantitative discussion of these results is given in an accompanying publication with detailed calculations of the expected <sup>41</sup>Ca/Ca ratios, also including modeling of the individual's shielding conditions (51).

Nonetheless, to provide a view of the quantitative results obtained in this study, the calculated <sup>41</sup>Ca/Ca ratios using DS02 (at a height of 1 m, free-in-air conditions; Table 1) and the results obtained here were included in Fig. 4 for comparison (dashed line). As can be seen, the calculated ratios decrease with increasing distance from the hypocenter, from  $2.2 \times 10^{-14}$  at 900 m to about  $0.3 \times 10^{-14}$  at 1,163 m, while the measured data give values of  $1.5 \times 10^{-14}$  at 900 m and about  $0.5 \times 10^{-14}$  at 1,163 m, respectively. Most of the observation points are below the curve for the calculated values except for three points at around 1,115 m that are slightly higher than the calculated values. The lower observed values within 1,020 m are most likely due to shielding effects of buildings or any other intervening materials, whereas the slightly higher ratios at the remote distance might be due to the limiting statistics associated with the <sup>41</sup>Ca measurements and/or presence of potential build-up materials (low-Z material such as water) that moderate fast neutrons effectively. These issues are discussed in detail in ref. (51).

## Conclusion

In the present study, a direct signal of exposure to A-bomb neutrons was detected for the first time by means of AMS of tooth samples from A-bomb survivors. Such signals are independent of survivor recall and provide a direct biological fingerprint of neutron exposure. In combination with the neutron energy spectrum during exposure, the measured  $^{41}\text{Ca}/\text{Ca}$  ratio provides a direct measure of neutron dose. Due to the expected low signals, a dedicated chemical sample preparation method was required to produce calcium hydride from the tooth enamel. Both AMS facilities used, the Munich tandem accelerator, which provides high particle energies in combination with a sophisticated particle-detection setup (GAMS), and the VERA facility permitted the measurement of  $^{41}\text{Ca}$  down to naturally occurring background levels. In comparison to the nonexposed survivors, those exposed to A-bomb radiation within 1,200 m of the hypocenter showed clearly higher  $^{41}\text{Ca}/\text{Ca}$  isotope ratios. In addition, decreasing  $^{41}\text{Ca}/\text{Ca}$  ratios were found in samples with exposures from increasing distances from the hypocenter, which is consistent with DS02 neutron transport calculations.

## ACKNOWLEDGMENTS

The authors are deeply indebted to the A-bomb survivors who donated their extracted teeth. Without their collaboration, the present study would not have been possible. The authors greatly appreciate Dr. H. M. Cullings for his efforts in collecting information concerning the exposure conditions of the tooth donors and Dr. Leon Kapp for his careful reading of the manuscript. This publication is partly based on research performed at the Radiation Effects Research Foundation (RERF), Hiroshima and Nagasaki, Japan. RERF is a private foundation funded by the Japanese Ministry of Health, Labor and Welfare, and the U.S. Department of Energy through the U.S. National Academy of Sciences. This publication was supported by RERF Research Protocol B-42.

Received: October 21, 2009; accepted: March 24, 2010; published online: May 25, 2010

## REFERENCES

1. D. L. Preston, Y. Shimizu, D. A. Pierce, A. Suyama and K. Mabuchi, Studies of mortality of atomic bomb survivors. Report 13: Solid cancer and noncancer disease mortality: 1950–1997. *Radiat. Res.* **160**, 381–407 (2003).
2. D. L. Preston, D. A. Pierce, Y. Shimizu, H. M. Cullings, S. Fujita, S. Funamoto and K. Kodama, Effect of recent changes in atomic bomb survivor dosimetry on cancer mortality risk estimates. *Radiat. Res.* **162**, 377–289 (2004).
3. D. L. Preston, E. Ron, S. Tokuoka, S. Funamoto, N. Nishi, M. Soda, K. Mabuchi and K. Kodama, Solid cancer incidence in atomic bomb survivors: 1958–1998. *Radiat. Res.* **168**, 1–64 (2007).
4. E. T. Arakawa, Radiation dosimetry in Hiroshima and Nagasaki atomic-bomb survivors. *New Eng. J. Med.* **263**, 488–493 (1960).
5. J. A. Auxier, J. S. Cheka, F. F. Haywood, T. D. Jones and J. H. Thorngate, Free-field radiation-dose distribution from the Hiroshima and Nagasaki bombings. *Health Phys.* **12**, 425–429 (1966).
6. W. C. Roesch, Ed., *US-Japan Joint Reassessment of Atomic Bomb Radiation Dosimetry in Hiroshima and Nagasaki – Final Report*, Vols. 1 and 2. Radiation Effects Research Foundation, Hiroshima, 1987.
7. R. W. Young and G. D. Kerr, Eds., *Reassessment of the Atomic Bomb Radiation Dosimetry for Hiroshima and Nagasaki: Dosimetry System DS02*, Vols. 1 and 2. Radiation Effects Research Foundation, Hiroshima, 2005.
8. F. Yamasaki and A. Sugimoto, Radioactive  $^{32}\text{P}$  produced in sulfur in Hiroshima. In *Collection of Investigative Reports on Atomic Bomb Disaster*, pp. 5–10. Science Council of Japan, Tokyo, 1953.
9. A. Sugimoto, Determination of number of fast neutron particles emitted at the time of the Hiroshima A-bomb explosion. In *Collection of Investigative Reports on Atomic Bomb Disaster*, pp. 18–19. Science Council of Japan, Tokyo, 1953.
10. B. Arakatsu, Report on survey of radioactivity in Hiroshima several days after the atomic bomb explosion. In *Collection of Investigative Reports on Atomic Bomb Disaster*, pp. 34–35. Science Council of Japan, Tokyo, 1953.
11. W. Rühm, A. M. Kellerer, G. Korschinek, T. Faestermann, K. Knie, G. Rugel, K. Kato and E. Nolte, The Dosimetry System DS86 and the neutron discrepancy in Hiroshima – historical review, present status, and future options. *Radiat. Environ. Biophys.* **37**, 293–310 (1998).
12. J. E. McAninch, L. J. Hainsworth, A. A. Marchetti, M. R. Leivers, P. R. Jones, A. E. Dunlop, R. Mauthe, J. S. Vogel, I. D. Proctor and T. Straume, Measurement of  $^{63}\text{Ni}$  and  $^{59}\text{Ni}$  by accelerator mass spectrometry using characteristic projectile X-rays. *Nucl. Instrum. Methods Phys. Res. B* **123**, 137–143 (1997).
13. A. A. Marchetti, L. J. Hainsworth, J. E. McAninch, M. R. Leivers, P. R. Jones, I. D. Proctor and T. Straume, Ultra-separation of nickel from copper metal for the measurement of  $^{63}\text{Ni}$  by AMS. *Nucl. Instrum. Methods Phys. Res. B* **123**, 230–234 (1997).
14. G. Rugel, T. Faestermann, K. Knie, G. Korschinek, A. A. Marchetti, J. E. McAninch, W. Rühm, T. Straume and C. Wallner, Accelerator mass spectrometry of  $^{63}\text{Ni}$  using a gas-filled magnet at the Munich tandem laboratory. *Nucl. Instrum. Methods Phys. Res. B* **172**, 934–938 (2000).
15. G. Rugel, A. Arazi, K. L. Carroll, T. Faestermann, K. Knie, G. Korschinek, A. A. Marchetti, R. E. Martinelli, J. E. McAninch and C. Wallner, Low level measurement of  $^{63}\text{Ni}$  by means of accelerator mass spectrometry. *Nucl. Instrum. Methods Phys. Res. B* **223–224**, 776–781 (2004).
16. W. Rühm, K. Knie, G. Rugel, T. Faestermann, A. A. Marchetti, J. E. McAninch, T. Straume, C. Wallner and G. Korschinek, Detection of  $^{63}\text{Ni}$  by means of accelerator mass spectrometry for estimating the fluence of fast neutrons from the Hiroshima atomic bomb. *Health Phys.* **79**, 358–364 (2000).
17. T. Straume, G. Rugel, A. A. Marchetti, W. Rühm, G. Korschinek, J. E. McAninch, K. Carroll, S. Egbert, T. Faestermann and C. Wallner, Measuring fast neutrons in Hiroshima at distances relevant to atomic-bomb survivors. *Nature* **424**, 539–542 (2003).
18. E. Nolte, W. Rühm, H. H. Loosli, I. Tolstikhin, K. Kato, T. C. Huber and S. D. Egbert, Measurements of fast neutrons in Hiroshima by use of  $^{39}\text{Ar}$ . *Radiat. Environ. Biophys.* **44**, 261–271 (2006).
19. K. Komura, M. Hoshi, S. Endo, T. Imanak and H. Fukushima, Ultra-low-background measurements of  $^{152}\text{Eu}$  in Hiroshima samples. In *Reassessment of the Atomic Bomb Radiation Dosimetry for Hiroshima and Nagasaki: Dosimetry System DS02* (R. W. Young and G. D. Kerr, Eds.), Vol. 2, pp. 588–592. Radiation Effects Research Foundation, Hiroshima, 2005.
20. Y. Nagashima, R. Seki, T. Matsuhiro, T. Takahashi, K. Sasa, K. Sueki, M. Hoshi, S. Fujita, K. Shizuma and H. Hasai, Chlorine-



- 36 in granite samples from the Hiroshima A-bomb site. *Nucl. Instrum. Methods Phys. Res. B* **223–224**, 782–787 (2004).
21. T. Straume, A. A. Marchetti, S. D. Egbert, J. A. Roberts, P. Men, S. Fujita, K. Shizuma and M. Hoshi, <sup>36</sup>Cl measurements in the United States. In *Reassessment of the Atomic Bomb Radiation Dosimetry for Hiroshima and Nagasaki: Dosimetry System DS02* (R. W. Young and G. D. Kerr, Eds.), Vol. 2, pp. 497–538. Radiation Effects Research Foundation, Hiroshima, 2005.
  22. T. Huber, W. Rühm, K. Kato, S. D. Egbert, F. Kubo, V. Lazarev and E. Nolte, The Hiroshima thermal-neutron discrepancy for <sup>36</sup>Cl at large distances. Part I: New <sup>36</sup>Cl measurements in granite samples exposed to A-bomb neutrons, *Radiat. Environ. Biophys.* **44**, 75–86 (2005).
  23. E. Nolte, T. Huber, W. Rühm, K. Kato, V. Lazarev and L. Schultz, The Hiroshima thermal-neutron discrepancy for <sup>36</sup>Cl at large distances. Part II: Natural in situ production as a source. *Radiat. Environ. Biophys.* **44**, 87–96 (2005).
  24. W. Rühm, T. Huber, K. Kato, S. D. Egbert and E. Nolte, <sup>36</sup>Cl measurements in Germany. In *Reassessment of the Atomic Bomb Radiation Dosimetry for Hiroshima and Nagasaki: Dosimetry System DS02* (R. W. Young and G. D. Kerr, Eds.), Vol. 2, pp. 539–554. Radiation Effects Research Foundation, Hiroshima, 2005.
  25. T. Straume, S. D. Egbert, W. A. Woolson, R. C. Finkel, P. W. Kubik, H. E. Gove, P. Sharma and M. Hoshi, Neutron discrepancies in the DS86 Hiroshima dosimetry system. *Health Phys.* **63**, 421–426 (1992).
  26. K. Shizuma, K. Iwatani, H. Hasai, M. Hoshi, T. Oka and H. Morishima, Residual <sup>152</sup>Eu and <sup>60</sup>Co activities induced by neutrons from the Hiroshima atomic bomb. *Health Phys.* **65**, 272–282 (1993).
  27. G. M. Raisbeck and F. Yiou, Possible use of <sup>41</sup>Ca for radioactive dating. *Nature* **277**, 42–44 (1979).
  28. D. Fink, R. Middleton, J. Klein and P. Sharma, <sup>41</sup>Ca: Measurement by accelerator mass spectrometry and applications. *Nucl. Instrum. Methods Phys. Res. B* **47**, 79–96 (1990).
  29. W. Kutschera, I. Ahmad, P. J. Billquist, B. G. Glasgola, K. Furer, R. C. Pardo, M. Paul, K. E. Rehm, P. J. Slota Jr., R. E. Taylor and J. L. Yntema, Studies towards a method for radiocalcium dating of bones. *Radiocarbon* **31**, 311–323 (1989).
  30. P. F. Rose, Ed., *ENDEIB-VI Summary Documentation*. Report BNL-NCS-17541, Nuclear Data Center, Brookhaven National Laboratory, Upton, NY, 1991.
  31. ICRP, *Basic Anatomical and Physiological Data for Use in Radiological Protection: Reference Values*. Publication 89, *Annals of the ICRP*, Elsevier, Amsterdam, 2003.
  32. A. A. Romanyukha, M. G. Mitch, Z. Lin, V. Nagy and B. M. Coursey, Mapping the distribution of <sup>90</sup>Sr in teeth with a photostimulable phosphor imaging detector. *Radiat. Res.* **157**, 341–349 (2002).
  33. E. I. Tolstykh, E. A. Shiskina, M. O. Degteva, D. V. Ivanov, S. N. Bayankin, L. R. Anspaugh, B. A. Napier, A. Wieser and P. Jacob, Age dependencies of <sup>90</sup>Sr incorporation in dental tissues: Comparative analysis and interpretation of different kinds of measurements obtained for residents on the Techa River. *Health Phys.* **85**, 409–419 (2003).
  34. H. J. Maier and W. Kutschera, Preparation of isotopically enriched sputter targets for the production of tandem accelerated beams of <sup>48</sup>Ca and <sup>14</sup>C. *Nucl. Instrum. Methods Phys. Res.* **167**, 91–96 (1979).
  35. G. M. Raisbeck, F. Yiou, A. Peghaire, J. Guillot and J. Uzureau, Instability of KH<sub>3</sub><sup>-</sup> and potential implications for detection of <sup>41</sup>Ca with a tandem electrostatic accelerator. In *Proceedings of the Symposium on Accelerator Mass Spectrometry* (W. Henning, W. Kutschera, R. K. Smither and J. L. Yntema, Eds.), p. 426. Report ANL/PHY-81-1, Argonne National Laboratory, Argonne, IL, 1981.
  36. A. Wallner, A. Arazi, T. Faestermann, K. Knie, G. Korschinek, H. J. Maier, N. Nakamura, W. Rühm and G. Rugel, <sup>41</sup>Ca – a possible neutron specific biomarker in tooth enamel. *Nucl. Instrum. Methods Phys. Res. B* **223–224**, 759–764 (2004).
  37. N. Nakamura, C. Miyazawa, S. Sawada, M. Akiyama and A. A. Awa, A close correlation between electron spin resonance (ESR) dosimetry from enamel and cytogenetic dosimetry from lymphocytes of Hiroshima atomic-bomb survivors. *Int. J. Radiat. Biol.* **73**, 619–627 (1998).
  38. G. Korschinek and W. Kutschera, A <sup>48</sup>Ca beam for tandem accelerators. *Nucl. Instrum. Methods Phys. Res.* **144**, 343–345 (1977).
  39. D. Fink, M. Paul and G. Hollos, Production of negative ion beams and sample preparation for <sup>41</sup>Ca accelerator mass spectrometry. In *Workshop on Techniques in Accelerator Mass Spectrometry* (R. E. M. Hedges and E. T. Hall, Eds.), pp. 23–33. Oxford University Press, Oxford, 1986.
  40. K. Knie, T. Faestermann and G. Korschinek, AMS at the Munich gas-filled analyzing magnet system GAMS. *Nucl. Instrum. Methods Phys. Res. B* **123**, 128–131 (1997).
  41. K. Knie, T. Faestermann, G. Korschinek, G. Rugel, W. Rühm and C. Wallner, High-sensitivity AMS for heavy nuclides at the Munich tandem accelerator. *Nucl. Instrum. Methods Phys. Res. B* **172**, 717–720 (2000).
  42. A. Wallner, M. Bichler, I. Dillmann, R. Golser, F. Käppler, W. Kutschera, M. Paul, A. Priller, P. Steier and C. Vockenhuber, AMS measurements of <sup>41</sup>Ca and <sup>55</sup>Fe at VERA – two radionuclides of astrophysical interest, *Nucl. Instrum. Methods Phys. Res. B* **259**, 677 (2007).
  43. A. Wallner, O. Forstner, R. Golser, G. Korschinek, W. Kutschera, A. Priller, P. Steier and C. Vockenhuber, Fluorides or hydrides? – <sup>41</sup>Ca performance at VERA’s 3-MV AMS facility. *Nucl. Instrum. Methods Phys. Res. B* **268**, 799–803 (2010).
  44. G. J. Feldman and R. D. Cousins, Unified approach to the classical statistical analysis of small signals. *Phys. Rev. D* **57**, 3873–3889 (1998).
  45. M. Paul, I. Ahmad and W. Kutschera, Half-life of <sup>41</sup>Ca. *Z. Phys. A* **340**, 249–254 (1991).
  46. W. Kutschera, I. Ahmad and M. Paul, Half-life determination of <sup>41</sup>Ca and some other radioisotopes. *Radiocarbon* **34**, 436–446 (1992).
  47. D. Fink, J. Klein and R. Middleton, <sup>41</sup>Ca: past, present and future. *Nucl. Instrum. Methods Phys. Res. B* **52**, 572–582 (1990).
  48. D. Müller, B. Bante, T. Faestermann, A. Gillitzer, H. J. Körner, G. Korschinek and U. Bittner, Accelerator mass spectrometry with a gas-filled magnetic spectrograph. *Nucl. Instrum. Methods Phys. Res. B* **68**, 313–318 (1992).
  49. G. Korschinek, H. Morinaga, E. Nolte, E. Preisnerberger, U. Ratzinger, A. Urban, P. Dragovitsch and S. Vogt, Accelerator mass spectrometry with completely stripped <sup>41</sup>Ca and <sup>53</sup>Mn ions at the Munich tandem accelerator. *Nucl. Instrum. Methods Phys. Res. B* **29**, 67–71 (1987).
  50. W. Rühm, K. Kato, G. Korschinek, H. Morinaga and E. Nolte, <sup>36</sup>Cl and <sup>41</sup>Ca depth profiles in a Hiroshima granite stone and the Dosimetry System 1986. *Z. Phys. A* **341**, 235–238 (1992).
  51. W. Rühm, A. Wallner, H. Cullings, S. D. Egbert, N. El-Faramawy, T. Faestermann, D. Kaul, K. Knie, G. Korschinek and G. Rugel, <sup>41</sup>Ca in tooth enamel. Part II: A means for retrospective biological neutron dosimetry in atomic bomb survivors. *Radiat. Res.* **174**, 146–154 (2010).